



Temperature effects on carbon mineralization of sinking copepod carcasses

Belén Franco-Cisterna^{1,*}, Peter Stief¹, Ronnie N. Glud^{1,2,3}

¹HADAL & Nordcee, Department of Biology, University of Southern Denmark, 5230 Odense, Denmark

²Department of Ocean and Environmental Sciences, Tokyo University of Marine Science and Technology, 108-8477 Tokyo, Japan

³Danish Institute for Advanced Study (DIAS), University of Southern Denmark, 5230 Odense, Denmark

ABSTRACT: Copepod carcasses are prevalent in marine ecosystems and might represent an important component of the sinking flux of particulate organic carbon in the ocean. The extent to which copepod carcasses contribute to the biological carbon pump is controlled by different environmental factors, including temperature. However, the effect of temperature on the longer-term kinetics of carbon mineralization of copepod carcasses is not well-studied. We conducted laboratory experiments to quantify the carbon mineralization associated with sinking carcasses of the cosmopolitan copepod *Acartia tonsa* through aerobic microbial respiration at 5 temperatures (20, 16, 12, 8, and 4°C). Microbial respiration rates associated with the carcasses were positively correlated with temperature and characterized by an initial short lag-phase, a rapid increase to a maximum rate, and a subsequent gradual decline in the rate of degradation. On average, 50% of the total carbon of the carcasses was mineralized within 6–12 d at 20°C, versus >60 d at 4°C. During the incubations, most carbon mineralization occurred in the ambient seawater, likely fueled by dissolved organic carbon leaking from the carcasses into the surrounding seawater. Extrapolating measured carbon turnover and sinking rates suggests that at 20°C, the mineralization of sinking copepod carcasses is constrained to the surface ocean. In contrast, at 4°C, sinking copepod carcasses can reach the deep ocean before they have been completely degraded. Hence, in low-temperature regions, copepod carcasses may represent an important agent for carbon export through the biological carbon pump.

KEY WORDS: Biological carbon pump · Marine snow · Copepods · *Acartia tonsa* · Temperature · Oxygen · Carbon · Degradation · Respiration

1. INTRODUCTION

The biological carbon pump mediates the vertical transport of organic material from the surface to the deep ocean, contributing to marine carbon sequestration (Turner 2015, Guidi et al. 2016). The efficiency of the pump to large extent depends on the abundance and composition of the plankton community in the surface water, and the mineralization of sinking particulate organic carbon (POC) during sinking towards deeper waters (Turner 2015). Fast-sinking particles, such as phytoplankton

aggregates and zooplankton fecal pellets, are commonly considered to be the main components of passive vertical POC fluxes (Steinberg et al. 2000, Turner 2015, Archibald et al. 2019). However, zooplankton carcasses might also represent an important source of sinking POC but, due to challenges in measuring the magnitude of the downward flux, they are often overlooked when assessing global carbon export from the surface ocean (Steinberg & Landry 2017).

Copepods are among the most abundant metazoans in the oceans (Mauchline 1998) and a key com-

*Corresponding author: belen@biology.sdu.dk

ponent in carbon cycling, transferring the carbon fixed by primary producers to higher trophic levels and to deep waters by active and passive transport (Steinberg et al. 2000, Saba et al. 2011, Steinberg & Landry 2017). Approximately 25–33% of copepod mortality is due to non-predatory factors (Hirst & Kiørboe 2002), producing carcasses which sink through the water column while being degraded by microorganisms. Sinking copepod carcasses are a source of labile substrates for bacterial degradation (Harding 1973, Tang et al. 2006b, Bickel & Tang 2010, Glud et al. 2015, Stief et al. 2017) and stimulate microbial production and enzymatic activity in the surrounding seawater (Tang et al. 2006b, 2009). To the extent copepod carcasses reach the seafloor, they serve as a source of organic matter for benthic food webs, and a fraction might ultimately be retained in the sediment record (Genin et al. 1995, Haury et al. 1995, Frangoulis et al. 2011). The fate of copepod carcasses will depend on different biological and physical factors affecting their degradation and sinking rates.

Temperature is the main physical variable controlling microbial respiration (Robinson 2019), microbial growth efficiency (Rivkin & Legendre 2001), POC attenuation (Iversen & Ploug 2013, Marsay et al. 2015, Belcher et al. 2016), and the large-scale structure of the ocean biological pump (Fakhraee et al. 2020). Carcass degradation has previously been described as a temperature-dependent process where the most labile material is lost from the carcasses on relatively short time scales of hours to weeks (Harding 1973, Lee & Fisher 1992, Tang et al. 2006a, Elliott et al. 2010). However, the applied methods have mainly been semi-quantitative based on the increase of carcass-associated bacterial density and visual changes of the carcasses (Harding 1973, Tang et al. 2006a). Quantification via loss of dry weight from the carcasses and the release of carcass-associated radiolabeled organic carbon has been done only for a maximum of 18 d (Lee & Fisher 1992, Elliott et al. 2010). Thus, the quantitative effect of temperature on the longer-term carcass degradation kinetics remains poorly explored.

A major challenge for experimental research on sinking copepod carcasses is how to generate dead specimens efficiently and reproducibly with the least effect on the copepod-attached microorganisms. In previous studies on copepod carcass degradation, different killing procedures have been applied. Among them, exposure to acetic acid (or other acids) has been commonly used (e.g. Glud et al. 2015, Tang et al. 2019a,b). However, the potential impact on the

performance of carcass-attached bacteria has not been fully considered.

The objectives of this study were to (1) define a killing method for producing copepod carcasses with minimal effects on the performance of carcass-attached bacteria, (2) quantify the effect of temperature on the mineralization of sinking copepod carcasses via aerobic microbial respiration, and (3) estimate the amount of POC which can be exported from the euphotic zone to deeper waters, using the cosmopolitan copepod *Acartia tonsa* as a model organism; based on our results, the potential quantitative contribution of copepod carcasses to the biological carbon pump is discussed.

2. MATERIALS AND METHODS

2.1. Culture of *Acartia tonsa*

Acartia tonsa is easy to culture and a very commonly used calanoid model species for laboratory investigations. It is globally distributed and dominant in zooplankton communities in temperate coastal regions (Cervetto et al. 1999, Escribano & Hidalgo 2000). Although *A. tonsa* is a coastal species, the results of carbon turnover rates during decomposition resolved in this study can be extrapolated to other open ocean copepods by considering the size and carbon content of the respective species.

Living specimens of the calanoid copepod *A. tonsa* were obtained from the Department of Science and Environment, Roskilde University, and kept in culture at the University of Southern Denmark. The cultures were established in 10 l tanks with 3 µm filtered and continuously aerated seawater at 16°C, salinity of 35, and under dark conditions. The animals were fed 2–3 times wk⁻¹ with a monoculture of the alga *Rhodomonas salina*.

2.2. Killing procedure for generating fresh copepod carcasses

Several procedures for producing zooplankton carcasses have previously been applied (Tang et al. 2019a and references therein). To explore the optimal method for producing carcasses with minimal impact on the performance of carcass-attached microbes, 3 different killing procedures were compared: acetic acid (10%) exposure for 10 s, freezing at –20°C for 1 h, and anoxia exposure for 2 h. Anoxia (<10 µmol O₂ l⁻¹) was produced by extensive flushing

of the seawater with N_2 and checked by measuring the O_2 concentration through an oxygen-sensitive optode patch (see below for details). The death of the animals was confirmed by the lack of movements upon stimulation, the lack of peristaltic gut movements, and the sinking to the bottom of the incubation vials even after exposure to fully oxic seawater for several hours.

Only female *A. tonsa* were used in the experiments; firstly, due to the observed female-skewed sex-ratio in copepod populations with a male/female ratio of ≤ 0.4 for *Acartia* species during most of the year (Kjørboe 2006) and secondly, to reduce variability in the carbon content of the carcasses since female *A. tonsa* are larger than males (Barata et al. 2002, Krause et al. 2017).

After producing the carcasses, aerobic microbial respiration was quantified for several days. To this end, 10 fresh carcasses each were transferred into a 6 ml glass vial with a gas-tight septum cap (i.e. exetainer, Labco), equipped with an internal, oxygen-sensitive optode patch (see below for details). The exetainers were filled with $0.2 \mu\text{m}$ filtered and air-saturated seawater, in 3–5 replicates treatment⁻¹ (i.e. killing procedure). Carcasses were incubated at 17°C and the oxygen concentration in the exetainers was measured at time intervals ranging from 2–12 h for 2 d (killing by anoxia) and 4.6 d (killing by freezing or acetic acid). The incubation period for the anoxic treatment was reduced as the ambient O_2 levels soon approached hypoxic conditions. The optimal procedure for carcass production was expected to result in high rates of respiration without any or with a relatively short lag-phase.

2.3. Carcass degradation experiments

2.3.1. Short-term experiments

Aerobic microbial respiration associated with decaying copepod carcasses was quantified as a proxy for carbon mineralization at incubation temperatures of 4, 8, 12, 16, and 20°C . For this procedure, 20 carcasses each of adult female *A. tonsa*, produced by anoxia exposure, were transferred into acid-washed 12 ml exetainers with air-saturated and $3 \mu\text{m}$ filtered seawater (5 replicates). Controls without carcasses were made with air-saturated and $3 \mu\text{m}$ filtered seawater (3 replicates). The exetainers were mounted on a plankton wheel rotating at $15 \text{ rounds min}^{-1}$ to simulate the sinking in the water column. The incubation temperatures were adjusted either in a thermoregu-

lated room or with the plankton wheel submerged in a thermoregulated water bath. The experiments were run in darkness for 2–10 d, depending on the incubation temperature (see Fig. S1 in the Supplement at www.int-res.com/articles/suppl/m679p031_supp.pdf). Incubations were terminated when hypoxic conditions (defined as $100 \mu\text{M } O_2$) were reached in the incubation vials.

To distinguish between respiration occurring directly associated with the carcasses and in the ambient seawater, at different time points 1 exetainer treatment⁻¹ was selected for dedicated experimentation. First, the carcasses were removed, and 1 ml of seawater was preserved with formaldehyde (final concentration 4%) for microbial abundance analysis (see below for details). To quantify respiration in the ambient seawater, 6 ml of the remaining seawater was transferred into an acid-washed 6 ml exetainer, re-oxygenated, and re-incubated for further respiration measurements. Respiration directly associated with the carcasses was calculated by subtracting the seawater-associated respiration from the total respiration measured just before sacrificing the exetainer. In the following sections, the different measurements/calculations of respiration/mineralization are termed 'total' when referring to the total activity in the incubation vial (i.e. carcasses + seawater) and 'carcass-associated' when referring to the activity calculated for the carcasses only (i.e. total — seawater).

2.3.2. Long-term experiments

To assess the amount of organic carbon of *A. tonsa* carcasses that can be oxidized by aerobic microbial respiration during descent, carcass incubations were run until respiration became extremely low. For this procedure, the experimental design described above was implemented with some modifications (Fig. S1): (1) instead of 20, only 10 fresh carcasses each were incubated in one 12 ml exetainer (6–7 replicates plus 3 controls without carcasses); (2) oxygen measurements were done every day; (3) at different time points defined by oxygen concentrations of $\sim 50\%$ air saturation (20°C) and $\sim 70\%$ air saturation (4 and 12°C), 1 exetainer treatment⁻¹ was sacrificed to determine the sinking speed of the carcasses and to quantify respiration in the seawater as before. At the same time point, the remaining exetainers with carcasses were carefully re-oxygenated until $>90\%$ air saturation to continue the incubations under oxic conditions. To this end, 1 ml of seawater of each exetainer was temporarily transferred into a sterile cen-

trifuge tube to create a headspace in the exetainer. This allowed the re-oxygenation of the remaining seawater by gently turning the exetainers upside down, thereby avoiding disruption of the carcasses. After a few turns, the exetainers were opened and exposed to the air, allowing for gas exchange. This procedure was repeated 3 times and then the water volume initially removed was put back into the exetainer to continue the incubation. These experiments were run at 20 and 12°C for 1 mo, and at 4°C for 2 mo to resolve the time required to almost complete degradation of sinking copepod carcasses and to allow extrapolation of the percentage of carbon turnover in copepod carcasses with slow descent rates and at great water depths.

2.4. Carbon loss from *A. tonsa* carcasses

Carbon loss from *A. tonsa* carcasses was estimated as the sum of carbon mineralized due to aerobic microbial respiration and carbon assimilated into biomass by bacteria. To measure oxygen concentration during the incubations, exetainers were equipped with an oxygen-sensitive optode on their inner side that could be interrogated from the outside by a FireSting Oxygen Meter (PyroScience). Respiration rates were calculated from the linear decrease in oxygen concentration in the incubation vials in defined time intervals during the entire incubation period. Results from both short- and long-term experiments were combined after standardization to the incubation volume and number of carcasses.

To quantify the amount of organic carbon per carcass that is mineralized by aerobic microbial respiration, total oxygen consumption was calculated and converted to carbon oxidation assuming theoretical respiratory quotients (RQs) ranging from 0.77–0.85, as reported for sinking detrital material (Wassmann 1984, Alkemade et al. 1992). Since a fraction of the carbon utilized by bacteria is assimilated into biomass, bacterial production (BP) was calculated assuming bacterial growth efficiencies (BGEs) of 5, 15, and 20% and the total measured aerobic bacterial respiration (BR), according to: $BP = (BGE \times BR) / (1 - BGE)$ (del Giorgio & Cole 1998). BGEs of 5 and 20% have been measured in oligotrophic and eutrophic environments, respectively (del Giorgio et al. 2011), while a BGE of 15% represents a reasonable marine average according to Kirchman et al. (2009).

Total cumulative carbon loss from the carcasses was calculated as the sum of daily total carbon consumption (i.e. carbon mineralization and bacterial

biomass production) and expressed relative to the total measured organic carbon content of fresh carcasses. The latter was quantified by an elemental analyzer coupled to an isotope ratio mass spectrometer (Delta V Advantage IRMS with Thermo Scientific EA) in 3 batches of 25 adult female *A. tonsa* each.

To estimate the percentage of mineralization taking place in the carcass itself, carcass-associated cumulative carbon loss was derived by subtracting daily carbon consumption in the ambient seawater from total carbon consumption. The obtained values were used to calculate the carcass/seawater mineralization ratio at 3 different temperatures (4, 12, and 20°C).

2.5. Other analyses

2.5.1. Microbial abundance

At different time points during the incubation experiments, 1 ml of seawater was taken for microbial abundance analysis. The samples were preserved with 100 µl formaldehyde 37% at 4°C overnight and then frozen at –20°C until flow cytometry analysis. For this procedure, the samples were thawed, stained with 2 µl of SYBR Green I for 20 min, and measured in a flow cytometer (BD FACSAria II cell sorter; BD Biosciences).

2.5.2. *In vitro* carcass sinking rates

Carcasses from the long-term experiments were used to measure sinking rates in the laboratory at different temperatures and degradation stages. Individually, carcasses of different ages were gently deposited in the center of the water surface in a graduated cylinder filled with 500 ml seawater equilibrated to 4, 14, and 17°C. The sinking rates were measured as the time it took for the carcass to descend 13 cm. The rates were extrapolated to $m d^{-1}$.

2.6. Statistical analysis

To detect a potential lag-phase in respiration caused by the different killing procedures, a 1-sample *t*-test (1-tailed) was used. Differences were determined if the initial respiration rate was significantly different from the detection limit of the respiration measurements, defined as 3 standard deviations of the average respiration rate in controls (i.e. $0.28 \mu M h^{-1}$).

To identify differences in the total respiration rates between the 3 killing procedures in 4 time intervals and the overall average of microbial abundances between different temperatures, 1-way ANOVA (2-tailed) was used followed by the Holm-Sidak post hoc test. This analysis was applied after testing that samples came from normally distributed populations with equal variances.

To identify differences in total respiration rates per time interval and the overall average of total and carcass-associated cumulative carbon loss between different temperatures, a non-parametric Kruskal-Wallis 1-way ANOVA on ranks analysis was used followed by the Dunn's post hoc test. Differences between total and carcasses-associated cumulative carbon loss were assessed by a non-parametric Mann-Whitney rank-sum test. These non-parametric tests were used when data were not normally distributed. All tests were performed at a significance level of $\alpha = 0.05$ in the statistical software SigmaPlot version 11.0.

3. RESULTS

3.1. Killing procedures

Three different killing procedures for generating fresh copepod carcasses were tested. The results were compared to identify the procedure that least affected the microbial respiration rates and avoided a lag-phase immediately after carcass production.

All 3 procedures resulted in low initial O_2 consumptions, followed by a period with a fast O_2 decline and a subsequent gradual attenuation in the O_2 consumption rate (Fig. 1A). During the first 2 h of incubation, all treatments exhibited very low total respiration rates ($<1.1 \text{ nmol } O_2 \text{ carcass}^{-1} \text{ h}^{-1}$). However, during the following 2–18 h of incubation, respiration rates differed significantly between the 3 killing procedures (Table S1, Fig. 1B). The anoxia treatment resulted in the highest respiration rates; more than 5-fold higher than the lowest rates measured for the acetic acid treatment. Total microbial respiration rates between 18 and 48 h appeared highest for carcasses produced by freezing and lowest for carcasses produced by acetic acid exposure, but the differences were not statically significant (Fig. 1B).

Copepod carcasses produced by acetic acid exposure exhibited a distinct lag-phase of 18 h, during which respiration was not significantly different from the detection limit of the respiration measurements (see Section 2.6 for details). Using the same statistical criterion, the freezing treatment exhibited a lag-

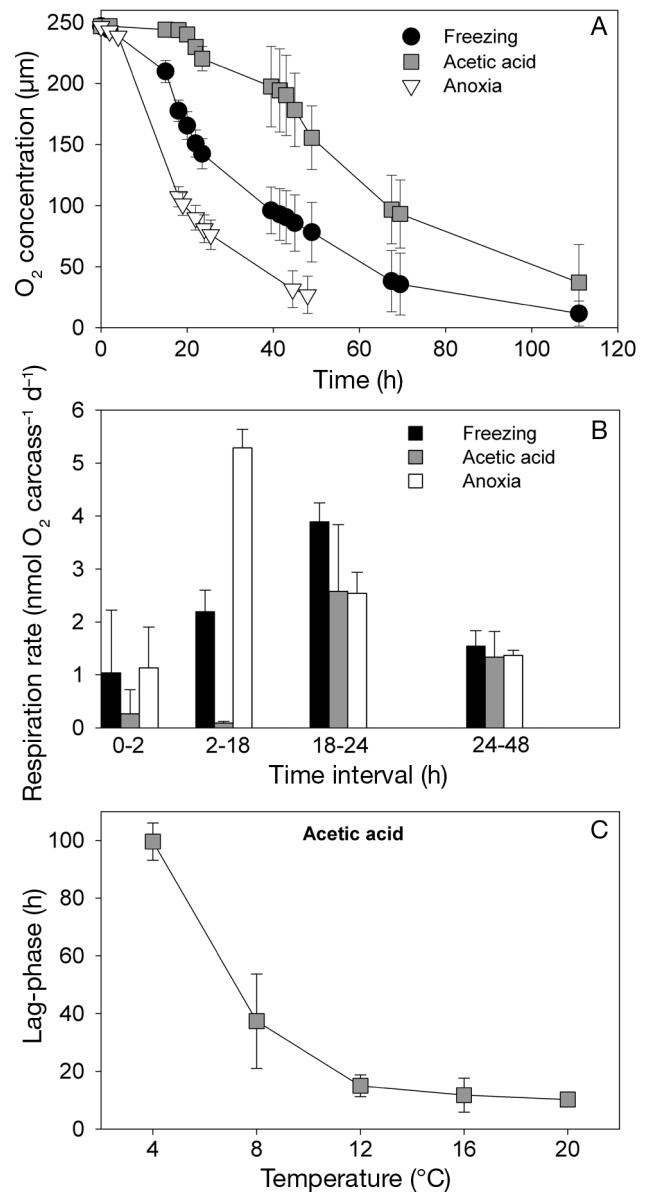


Fig. 1. Evaluation of killing procedures for producing carcasses of the copepod *Acartia tonsa*. (A) Oxygen concentration over time in incubations with carcasses produced by freezing, acetic acid exposure, and anoxia exposure at 17°C. Means \pm SD of 3–5 incubations with 10 carcasses each are shown. (B) Rates of total aerobic microbial respiration associated with carcasses produced by freezing, acetic acid exposure, and anoxia exposure. Means \pm SD of rates from 3–5 incubations with 10 carcasses each are shown. (C) Lag-phase before observing a decline in O_2 concentration following a treatment with acetic acid as a function of temperature (4, 8, 12, 16, 20°C). Means \pm SD from 5 incubations with 20 carcasses each are shown

phase of 2 h, and only an insignificant lag-phase was observed in the anoxia treatment (Fig. 1A). Data compiled from experiments with carcasses produced by acetic acid exposure at different temperatures further

revealed an inverse correlation between the length of the lag-phase and the ambient temperature (Fig. 1C). At 4°C, the lag-phase extended up to 4 d before respiration rates reached values different from the detection limit of the respiration measurements. Based on these observations, we decided to apply *Acartia tonsa* carcasses that were produced by exposure to anoxia.

3.2. Carcass degradation

Aerobic microbial respiration associated with degrading copepod carcasses was measured in both short-term (up to 10 d) and long-term (up to 60 d) incubations. The results from the 2 incubation procedures were combined.

Total aerobic respiration rates associated with *A. tonsa* carcasses were initially low, followed by a period with the maximum activity and a gradual attenuation in the resolved rates (Fig. 2). The same pattern was observed at all temperatures but at different rates and with different lengths of the respective phases (Fig. S2). Total respiration rates were positively correlated with temperature and significantly different between higher and lower temperatures during the first week of incubation (Table S2).

The time to reach maximum activity was inversely correlated with temperature (Fig. 2). At higher temperatures, 20 and 16°C, maximum total respiration rates were measured on the first day of degradation, whereas at lower temperatures, 8 and 4°C, maximum rates were measured on Days 3 and 6, respectively.

3.3. Microbial abundance

Carcass degradation promoted the growth of free-living bacteria in the surrounding seawater, and bacterial growth was positively correlated with temperature in both short- and long-term experiments. Microbial abundances increased from $>10^6$ cells ml⁻¹ to peak abundances of $>10^8$ cells ml⁻¹ at 20 and 16°C (Fig. 2A,B), in contrast to $>10^7$ cells ml⁻¹ at 12, 8, and 4°C (Fig. 2C,D,E). The time to reach the peak in microbial abundance was inversely correlated with temperature. At 20 and 16°C, maximum microbial abundances were observed in the first 2 d of incubation, followed by 2–3 d at 12 and 8°C, and 8 d at 4°C. After the peak, a decrease in the abundances to values close to the initial numbers was observed. Abundances in controls without carcasses remained constant during the incubations ($\sim 10^6$ cells ml⁻¹) at all temperatures (Fig. 2).

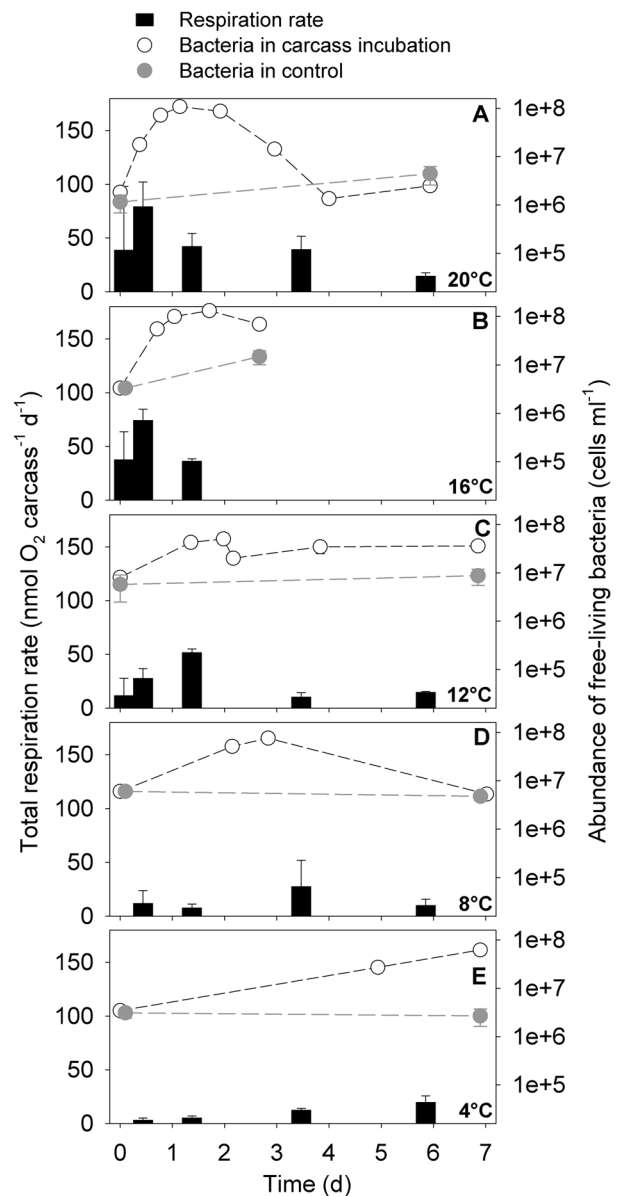


Fig. 2. Total respiration rate (bars) and abundance of free-living bacteria in *Acartia tonsa* carcass incubations (white dots) and controls (grey dots) during short-term experiments at (A) 20°C, (B) 16°C, (C) 12°C, (D) 8°C, and (E) 4°C. For respiration rates, means \pm SD of 5 replicate incubations with 20 carcasses each are shown; (A,C,E) also include 6–7 replicates from long-term incubations. For the abundance of free-living bacteria, means \pm SD of 1–4 replicates are shown

3.4. Carbon loss from *A. tonsa* carcasses

The independently determined total carbon content of fresh, female *A. tonsa* carcasses was 6.97 ± 1.06 $\mu\text{g C carcass}^{-1}$. Loss of organic carbon from the copepod carcasses was estimated from aerobic respiration (BR) and BP at all temperatures in both the

short- and long-term experiments. The cumulative amount of organic carbon lost from the carcasses was positively correlated with temperature (Fig. 3). During the first 25 d of oxic incubations, $84 \pm 11\%$ of the total carbon content of the carcasses was lost due to mineralization and bacterial biomass production at 20°C (Fig. 3A), followed by significantly lower percentages of $52 \pm 7\%$ and $26 \pm 3\%$ at 12°C (Fig. 3B) and 4°C (Fig. 3C), respectively (Table S3).

However, during the incubations, not all respiration activity was directly associated with the carcasses, as their degradation stimulated microbial activity in ambient seawater as well. A significantly lower contribution to total carbon loss by carcass-associated mineralization was generally observed at all temperatures (Table S4). During 25 d of degradation, up to $18 \pm 2\%$ of the total carbon content per carcass was mineralized directly on the carcasses at 20°C (Fig. 3D), followed by lower percentages of 14 ± 2 and $4 \pm 1\%$ at 12°C (Fig. 3E) and 4°C (Fig. 3F), respectively (Table S3).

The carcass/seawater mineralization ratio tended to increment until a peak close to 1, followed by a de-

crease to values lower than 1 (Fig. 4). This means that most of the microbial activity was occurring in the surrounding seawater at all temperatures and times.

At the end of the long-term incubations, when mineralization rates became extremely low, the calculated amount of organic carbon remaining in the carcasses was up to 1 ± 1 , 3 ± 1 , and $4 \pm 0.4 \mu\text{g C carcass}^{-1}$ at 20, 12, and 4°C , respectively. This is equivalent to 14 ± 12 , 47 ± 8 , and $55 \pm 6\%$ of the total organic carbon at 20, 12, and 4°C , respectively.

3.5. *In vitro* carcass sinking rates

The sinking rates of the carcasses were positively correlated with temperature and negatively correlated with carcass age (Fig. 5). Fresh carcasses sank at rates of $\sim 90 \text{ m d}^{-1}$ at 14 and 17°C and $\sim 60 \text{ m d}^{-1}$ at 4°C . After a few days of aging, the sinking rates decreased distinctly and reached a lower stable level of $\sim 60 \text{ m d}^{-1}$ at 17 and 14°C , and $\sim 20 \text{ m d}^{-1}$ at 4°C .

4. DISCUSSION

4.1. Killing procedure

An essential aspect to consider when performing experiments about copepod carcass degradation is the production of reproducible carcasses without affecting the performance of carcass-associated microorganisms. Previous studies on copepod carcass degradation commonly used acetic acid exposure for killing copepods. However, this study on *Acartia tonsa* carcasses revealed that microbial performance is negatively affected by short acetic acid exposure, inducing a long lag-phase with almost no microbial activity and the lowest respiration rates compared to carcasses produced by freezing and anoxia exposure. Acetic acid in lower concentrations (3%) is an effective bactericidal and antiseptic agent, probably due to physical alteration of the bacterial cell wall (Ryssel et al. 2009). Additionally, microbial enzymatic activity can be inhibited by acid exposure, leading to a decrease in the decomposition rates of organic matter (Kok & Van der Velde 1991).

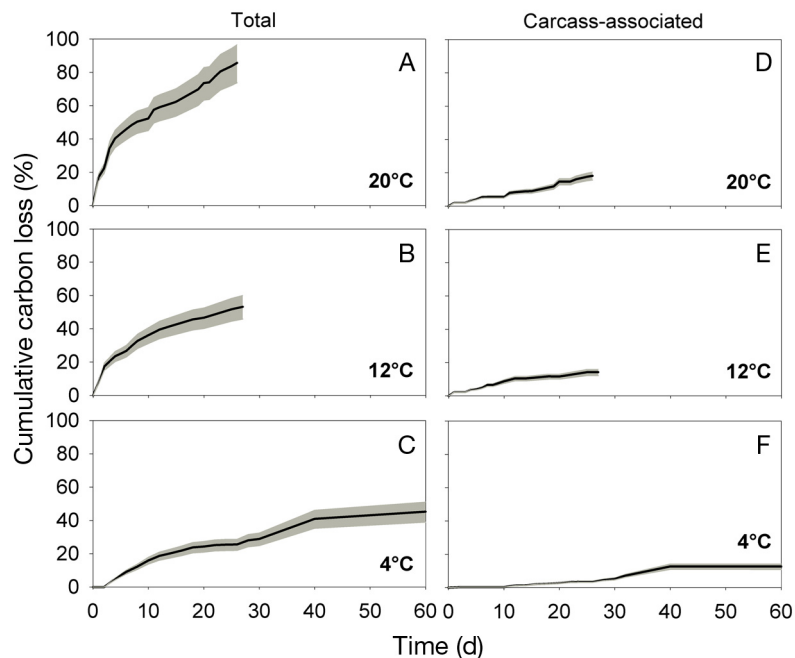


Fig. 3. Cumulative carbon loss from carcasses of the copepod *Acartia tonsa*. Total cumulative carbon loss derived from the daily total respiration and bacterial production in the incubation vials at (A) 20°C , (B) 12°C , and (C) 4°C . Carcass-associated cumulative carbon loss derived from subtraction of respiration and bacterial production in seawater from the total at (D) 20°C , (E) 12°C , and (F) 4°C . Black lines: cumulative carbon loss estimated with respiratory quotient (RQ) = 0.8 and bacterial growth efficiency (BGE) = 15%. Shaded areas: range in cumulative carbon loss estimated with RQs = 0.77 or 0.85 and BGEs = 5 or 20%

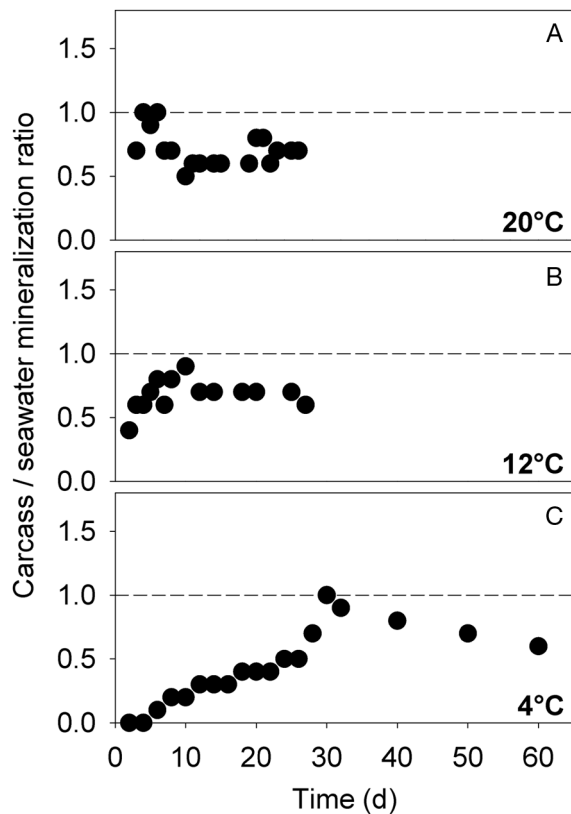


Fig. 4. Carcass/seawater mineralization ratio at (A) 20°C, (B) 12°C, and (C) 4°C. Dashed lines indicate a ratio of 1, meaning that equal proportions of the mineralization take place in the *Acartia tonsa* carcass and the surrounding seawater

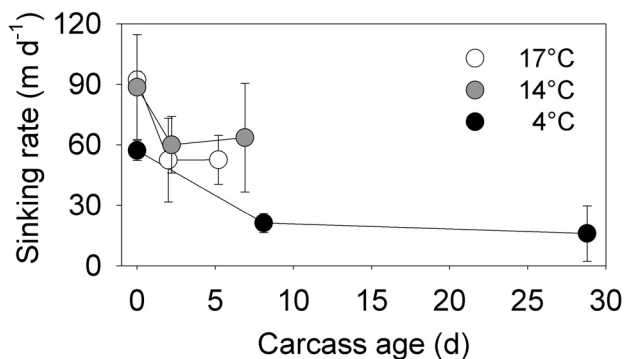


Fig. 5. *In vitro* sinking rates of *Acartia tonsa* carcasses as a function of temperature (17, 14, and 4°C) and carcass age. Means \pm SD of sinking rates from 3–7 carcasses are shown

Killing copepods by freezing resulted in a short lag-phase and higher respiration rates than acetic acid exposure (Fig. 1A,B). However, rapid freezing can induce bacterial death (Haines 1938, Mazur 1984) and the release of dissolved organic carbon (DOC) from both bacteria and copepods due to mechanical disruption of cells and tissues during freez-

ing. The decrease of carcass-associated bacterial abundance and stimulation of ambient communities by DOC leakage may induce severe changes in the resolved mineralization dynamics.

Carcasses produced by anoxia exposure not only exhibited the shortest lag-phase and relatively high respiration rates, but they also maintained intact carapace and internal tissues. These characteristics are most likely found in carcasses naturally produced by starvation, infections, and adverse environmental conditions (Daase et al. 2014). Natural mortality can also be induced by, among others, sloppy feeding by predators (Tang & Elliott 2014 and references therein), with severe consequences for the physical integrity of the carcasses. Thus, experimental exposure to anoxia may select for certain carcass features while naturally occurring carcasses might differ considerably, but for generating reproducible carcasses with a minimum impact on the copepod-associated microbial communities, we consider it to be the best approach.

4.2. Temperature dependence of carcass degradation

Mineralization of POC, including sinking copepod carcasses, is initiated by an intense exoenzymatic activity of POC-attached bacteria (Sempéré et al. 2000). At low temperatures, enzymatic activities are slowed down, and the reduced fluidity of cell membranes may further decrease the activity of membrane-bound transporter enzymes (Nedwell 1999). Combined with reduced cell-specific metabolic activity, carcass degradation is thus expected to decrease significantly with declining temperature. This hypothesis is supported by the current study, where microbial respiration exhibited a positive correlation with temperature, and 50% of the total organic material in carcasses of *A. tonsa* was mineralized after 60 d at 4°C, while the corresponding value was reached after 6–12 d at 20°C.

The temperature effect on copepod carcass degradation has been previously investigated applying a number of different methodologies (Table 1). The obtained rates of carbon turnover during the first day of degradation vary between 7.8 and 100% C d⁻¹ at temperatures close to 20°C and between 0.0 and 39.0% C d⁻¹ at temperatures below 8°C (Table 1). These variations at the respective temperatures might partly relate to the fact that the individual studies applied different copepod species, experimental procedures, and experimental conditions.

Table 1. Reported rates of copepod carcass degradation and carbon loss in marine ecosystems at different temperatures. MR: microbial respiration; BP: bacterial production

Copepod species	Study site(s)	Method	Temp. (°C)	Carcass degradation on Day 1	Time to reach 50% degradation (d)	Length of experiment (d)	Reference
<i>Calanus finmarchicus</i>	Sargasso Sea	Observation of copepod tissues and bacterial colonization	22	Only muscle tissues recognizable. Carcasses highly covered by bacteria	1	9	Harding (1973)
	Halifax		4	Small colonies of bacteria	5	11	
<i>Acartia tonsa</i>	Lower Chesapeake Bay	Observation of copepod tissues and bacterial colonization	30	> 70% of carcass covered by bacteria	0.5–1.3	7.3	Tang et al. (2006a)
	Long Island	¹⁴ C-carbon loss as DO ¹⁴ C and ¹⁴ CO ₂ over time	20 10 18	30–70% of carcass covered by bacteria Up to 30% of carcass covered by bacteria 32.0–47.0% C-turnover d ⁻¹	1.3–2.3 4.2 1.8–2.0	7.3 7.3 18	Lee & Fisher (1992)
<i>Acartia tonsa</i>	York River estuary	Loss of carcass dry weight over time	2 25	29.0–39.0% C-turnover d ⁻¹ 96.3% C-turnover d ^{-1d}	7.5–8.2 0.4	18 1.3	Elliott et al. (2010)
	Godthåbsfjord	Carbon loss derived from MR and BP	15 5	30.0% C-turnover d ^{-1d} 13.9% C-turnover d ^{-1d}	2 4.8	3 4.8	
Copepod community	Golfo Dulce	Carbon loss derived from MR and BP	7	1.9 ± 0.0004% C-turnover d ^{-1a, b}	27.0 ^c	3.3	Glud et al. (2015)
	North Atlantic subtropical convergence zone	Carbon loss derived from MR and BP	26	8.0 ± 0.8% C-turnover d ^{-1a}	6.2 ^c	1	Stief et al. (2017)
<i>Oithona</i> sp.	Sagami Bai	Carbon loss derived from MR and BP	22	7.8–39.5% C-turnover d ^{-1a}	1.3–6.4 ^c	1	Tang et al. (2019a)
<i>Acartia tonsa</i>	Culture	Carbon loss derived from MR and BP	26	7.8% C-turnover h ^{-1a}	0.3 ^c	0.1	Tang et al. (2019b)
			20	17.0% C-turnover d ⁻¹	8	26	This study
			16	7.3% C-turnover d ⁻¹	7.7	2.7	
			12	7.9% C-turnover d ⁻¹	25	2.7	
		8	0.9% C-turnover d ⁻¹	32.4	7.9		
			4	0.0% C-turnover d ⁻¹	> 60.0	61	

^aCarbon turnover rates calculated from the reported respiration rates

^bTotal carbon content per carcass obtained from literature

^cTime to reach 50% of degradation extrapolated from the reported or calculated C-turnover rates on Day 1

^dCarbon turnover rates calculated from loss of dry weight at Day 1 relative to the dry weight of carcass at 0.25 h since copepod death

One set of studies used microscopic observations of copepod tissues and bacterial colonization to assess the degradation stages. The observations suggested considerably faster degradation than in our study, i.e. 50% degradation after 0.5 d at 30°C (Tang et al. 2006a) and 5 d at 4°C (Harding 1973) (Table 1). While this semi-quantitative approach provides direct first-hand information on the tissue status and the advancement of microbial colonization, it only provides indirect information about carbon turnover rates. Therefore, the degradation kinetics are inferred from more subjective criteria in comparison with quantitative methods.

Other approaches for assessing degradation of *A. tonsa* carcasses were developed by Lee & Fisher (1992) by quantifying carbon loss from radiolabeled copepod carcasses and Elliott et al. (2010) via quantification of mass loss from copepod carcasses. Both studies concluded a positive correlation between carcass degradation and temperature and defined the course of decomposition as rapid at first and more slowly as time progressed. The results of this study agree with those observations; however, the rates of carbon turnover differ between the studies. On the first day of degradation, Lee & Fisher (1992) reported carbon loss rates—expressed as the sum of $^{14}\text{CO}_2$ production and the DO^{14}C release—from ^{14}C -labeled *A. tonsa* carcasses ca. 2.5-fold higher at 18°C and >14-fold higher at 2°C than the rates obtained at 20°C and 4°C, respectively, in the current study (Table 1). Thus, those authors concluded that 50% of the total carbon of *A. tonsa* carcasses is lost after 2 and 8 d at 18 and 2°C, respectively. Faster decomposition rates were measured by Elliott et al. (2010) where 50% of carcass dry weight loss occurred within 0.4 d after death at 25°C and ca. 5 d at 5°C, meaning that their carbon turnover rates were 20-fold higher at 25°C and 12-fold higher at 5°C than those obtained at 20 and 4°C, respectively, in the present study (Table 1). However, when only considering $^{14}\text{CO}_2$ production as an indicator of carbon mineralization, the rates measured by Lee & Fisher (1992) during the first day of degradation were 22 and 0.5% C d^{-1} at 18 and 2°C, respectively, and thus close to our measurements. This suggests that the overall higher carbon turnover rates reported from the radiotracer approach, and probably from the mass loss approach, could be related to the leakage of non-respired DOC fraction which is not included in our measurements as mineralized organic material. Thus, total carbon loss from the carcasses might be underestimated in our study during the first stages of degradation when DOC leaking from the

carcasses is high (Lee & Fisher 1992). The assumption that all copepod tissues were uniformly labeled can also result in an overestimation of carbon loss in the radiotracer approach, as higher labeled and labile POC might be degraded in the initial stages of the incubation.

More recently, microbial O_2 consumption associated with decaying carcasses has been measured as a quantitative proxy for carbon mineralization (Table 1). Aerobic respiration rates reported in the literature were converted in the current study to carbon mineralization and BP, assuming $\text{RQ} = 0.8$ and a $\text{BGE} = 15\%$, respectively (Table 1). At temperatures close to 20°C, the carbon turnover rates measured in the current study appear within the lower range of the values obtained in previous studies. In contrast, the only study made at low temperature (Glud et al. 2015) showed carbon turnover rates consistent with the values of the present study, i.e. 1.9% C d^{-1} at 7–8°C.

The variability in carbon turnover rates between respiration-based studies is partly related to the length of the incubations. Since long-term dynamics of carcass degradation was not the aim of previous studies, most of the respiration measurements were performed in short time-intervals (a few hours) and then extrapolated to 24 h. However, the current study has consistently shown a systematic decline in respiration rates at longer incubation times at all temperatures. Therefore, the higher carbon turnover rates from some previous studies may represent an overestimation resulting from linear extrapolation of respiration rates from short-term measurements.

The amount of total carbon per carcass critically affects the calculated carbon turnover rates. The studies listed in Table 1 either measured the carbon content of the carcasses directly (as in the current study) or estimated carbon content based on copepod body volume or dry weight. The highest carbon turnover rates were found in studies in which total carbon contents were estimated indirectly (e.g. Tang et al. 2019b). Additionally, the content and lability of organic carbon vary among zooplankton species (Bickel & Tang 2010); even the same species might show seasonal variation in, for instance, their lipid content (Sargent & Falk-Petersen 1988). The amount and nature of lipids, proteins, and carbohydrates affect the organic material lability, and this is expected to translate into variable degradation kinetics of the respective carcasses (Wakeham et al. 1997).

The microbial abundance in the seawater surrounding the decaying carcasses can also cause variation in the resolved total respiration rates from dif-

ferent incubation approaches. The studies cited in Table 1 utilized different filtration strategies, applying from 0.7–100 μm mesh size. This may have resulted in different ambient bacterial abundances and community compositions, including larger organisms (e.g. protozoans) in the incubation vials. This can lead to variation in carbon turnover rates since the current study has demonstrated that carcass degradation is also mediated by the ambient community (see below).

In the present study, carbon turnover rates derived from microbial respiration rates varied by less than 25%, applying a reasonable range of RQs and BGEs (Fig. 3). Thus, we consider continuous oxygen measurements during long-term incubations a strong tool for assessing the degradation dynamics of sinking copepod carcasses in natural settings. The current study resolved low carcass degradation rates at temperatures that prevail below the surface ocean (2–4°C) and indicates a larger potential for POC export through copepod carcasses than previously recognized.

4.3. Mineralization in the carcasses versus seawater

The carcass degradation experiments with *A. tonsa* revealed that respiration activity was in part directly associated with the carcasses and in part located in the ambient seawater. This finding suggests that microbial activity and growth in ambient seawater may have been stimulated by DOC and dissolved organic nitrogen released from the carcasses (Stief et al. 2018) (Fig. 6A). After the initial stimulation of microbial activity and growth in ambient seawater, microbial abundance declined in incubations at all temperatures. This decline was presumably related to viral lysis (Proctor & Fuhrman 1991), bacterivorous protozoans (Grossart & Ploug 2000), and/or the exhaustion of labile substrates.

The experimental approach utilized in this study differs from *in situ* settings. In natural conditions, copepod carcasses are not constrained to a small volume; therefore, the volume-specific consumption rates of DOC will be smaller than in the incubation

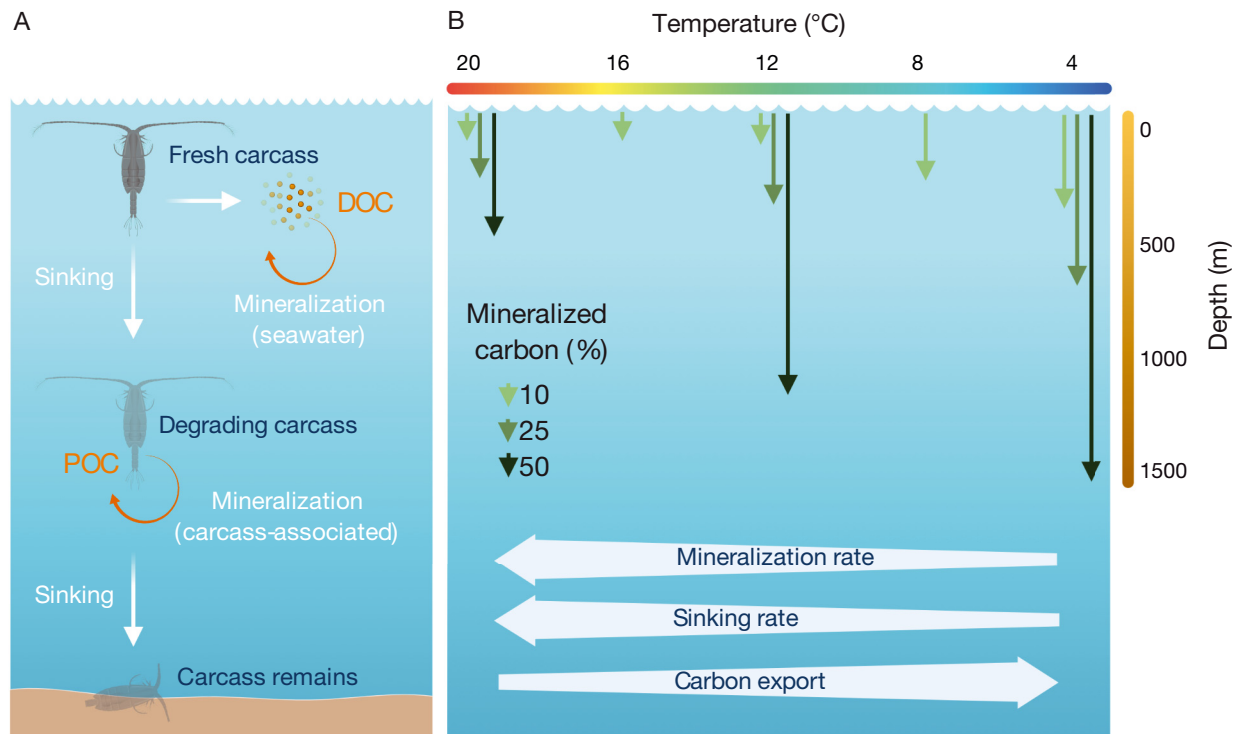


Fig. 6. Conceptual scheme of carbon mineralization associated with sinking carcasses of the copepod *Acartia tonsa* in the ocean as controlled by temperature. (A) Copepod carcass mineralization while sinking through the water column. (B) Total carbon export associated with copepod carcasses as a function of temperature. Vertical arrows: depth reached for one carcass when 10, 25, and 50% of its total carbon has been mineralized. Extrapolations at 20, 12, and 4°C were derived from long-term experiments; extrapolations at 16 and 8°C were derived from short-term experiments. Horizontal arrows: influence of temperature on the strength of the respective process. Created with <https://BioRender.com>

vials due to dilution in the water column. Indeed, we cannot exclude that the dilution can be so extensive that a fraction of the otherwise labile DOC will behave as a recalcitrant fraction (Arrieta et al. 2015). But it can be expected that most of the DOC leaked from the carcasses will be rapidly mineralized to CO₂ (Lee & Fisher 1992); hence, we consider the experimental conditions of this study still to represent a valid approach for assessing carbon cycling associated with sinking copepod carcasses.

4.4. Importance of sinking copepod carcasses for oceanic carbon cycling

The efficiency of the biological pump depends on the depth at which the sinking organic carbon is respired (Middelburg 2019). Thus, to estimate how much carbon from sinking copepod carcasses is aerobically mineralized and to assess how deep the carcass-associated organic carbon can reach, we numerically extrapolated our measurements. Percentages of carbon loss were resolved by respiration rates and BP in our incubation experiments and from the quantified total carbon content per carcass. This approach partly ignores potential anaerobic degradation, via for instance denitrification, which might be important in larger zooplankton species (Glud et al. 2015, Stief et al. 2017) but presumably not in smaller species such as *A. tonsa* (Ploug et al. 1997).

A. tonsa is a cosmopolitan copepod inhabiting the surface waters (0–100 m) of the coastal ocean in temperate regions, where it lives at temperatures between 9 and 30°C. Considering an adult population of 1992–13 965 ind. m⁻² (Criales-Hernández et al. 2008, Pino-Pinuer et al. 2014) and a rate of non-predatory mortality of 0.46 d⁻¹ (Yáñez et al. 2019), *A. tonsa* populations alone could cause a sinking flux of carcasses of between 916 and 6424 carcasses m⁻² d⁻¹, equivalent to a sinking flux of POC of 6.4–44.7 mg C m⁻² d⁻¹. Since this POC flux occurs in shallow areas (<200 m) and considering a sinking speed of 90 m d⁻¹, more than 70% of the total carbon of the carcasses can reach the seafloor in coastal areas, irrespective of temperature. Once settled on the sediments, the remains of the carcasses can either fuel the benthic food webs or be retained in the sedimentary record. This extrapolation relies on the assumption of specific abundances, mortality rates, and flux of sinking carcasses for a population in a steady state. Therefore, habitat-specific values of those parameters will affect the derived amounts

of exported organic carbon associated with *A. tonsa* carcasses.

To extrapolate our results to an oceanic context, we assumed that the degradation and sinking dynamics of our model organism could be applied to oceanic copepods. Assessments of carbon export were done based on the time needed to degrade 10, 25, and 50% of total carbon content per carcass and measured sinking rates (Fig. 6B). The calculations revealed that 10% of the total carbon is lost from the carcasses, due to mineralization and BP, in the first 90 m of the water column at 20, 16, and 12°C, while this threshold is first reached at 350–450 m at 8 and 4°C. Thus, at lower temperatures, 90% of the total carbon per carcass escapes degradation in the euphotic zone. The next 40% of the total carbon is lost within 400–700 m depth at 20°C, 1100–1700 m depth at 12°C, and >1400 m at 4°C, implying that 50% of organic material associated with the carcasses can be exported from the surface waters to the ocean interior at temperatures below 12°C (Fig. 6B). Once the carcasses have crossed the mesopelagic zone, the remaining POC is probably of low reactivity due to advanced carcass degradation. Mineralization and sinking rates also decline to very low levels of <1.4 nmol C carcass⁻¹ d⁻¹ and <20 m d⁻¹, respectively. Thus, the remaining POC from the copepod carcasses can sink slowly, almost unchanged, to the bathypelagic and abyssopelagic zones.

The calculations are expressed in percentages of carbon loss from copepod carcasses. Thus, this extrapolation can be applied to different copepod species. However, the absolute amount of carbon lost from the carcasses, the exported carbon, and the sinking rates may vary according to copepod size. We fully recognize that this is a first approximation and that many environmental variables other than temperature and sinking rates may affect the carbon export associated with sinking copepod carcasses. These include fragmentation and feeding of sinking carcasses by metazoans (Elliott et al. 2010), hydrodynamic conditions (Kirillin et al. 2012), and hydrostatic pressure effects on microbial communities (Tamburini et al. 2009, Stief et al. 2021). For further refinement of our assessment, such factors could be considered.

In the open ocean, imbalances between POC flux and the mesopelagic and benthic carbon demand have been documented (Baltar et al. 2009, Burd et al. 2010, Wiedmann et al. 2020), indicating the existence of unaccounted sources of organic carbon. Our study shows that reduced temperature facili-

tates the export of carcass-associated organic material to great depths and, potentially, even deep-sea sediments, where it can contribute to the sustenance of deep-ocean communities. Indeed, intact copepod carcasses have been found in high abundance in the mesopelagic and bathypelagic zones (200–2000 m), in some cases overtaking the abundance of live organisms (Daase et al. 2014, Tang et al. 2019a,b, Daase & Søreide 2021). Furthermore, copepod carcasses have been quantified in sediment traps deployed in the Arctic ocean, accounting for up to 91% of the POC flux (Sampei et al. 2009, 2012, 2020), but such carcasses are often considered to be ‘swimmers’ and are eliminated from the assessments. Thus, sinking copepod carcasses may represent an important component of the passive carbon flux in cold waters, and must therefore be considered when estimating the oceanic export flux of POC.

Acknowledgements. The authors thank Per Meyer Jepsen (Roskilde University, Denmark) for providing copepods for the experiments and Anni Glud, Rie Pors, and Erik Laursen for their technical support during the experimental activities. Thanks to Kam W. Tang, Eva Friis Møller, and the reviewers for their valuable comments to improve the manuscript. This work was funded by HADES-ERC Advanced Grant (No. 669947), the Danish National Research Foundation through the Danish Center for Hadal Research, HADAL (No. DNR145) awarded to R.N.G., and the National Agency for Research and Development (ANID), Scholarship Program, Doctorado Becas Chile, 2017-72180314 awarded to B.F.C.

LITERATURE CITED

- Alkemade R, Wielemaker A, de Jong SA, Sandee AJJ (1992) Experimental evidence for the role of bioturbation by the marine nematode *Diplolaimella dievengatensis* in stimulating the mineralization of *Spartina anglica* detritus. *Mar Ecol Prog Ser* 90:149–155
- Archibald KM, Siegel DA, Doney SC (2019) Modeling the impact of zooplankton diel vertical migration on the carbon export flux of the biological pump. *Global Biogeochem Cycles* 33:181–199
- Arrieta JM, Mayol E, Hansman RL, Herndl GJ, Dittmar T, Duarte CM (2015) Dilution limits dissolved organic carbon utilization in the deep ocean. *Science* 348:331–333
- Baltar F, Aristegui J, Gasol JM, Sintes E, Herndl GJ (2009) Evidence of prokaryotic metabolism on suspended particulate organic matter in the dark waters of the subtropical North Atlantic. *Limnol Oceanogr* 54:182–193
- Barata C, Medina M, Telfer T, Baird DJ (2002) Determining demographic effects of cypermethrin in the marine copepod *Acartia tonsa*: stage-specific short tests versus life-table tests. *Arch Environ Contam Toxicol* 43:373–378
- Belcher A, Iversen M, Manno C, Henson SA, Tarling GA, Sanders R (2016) The role of particle associated microbes in remineralization of fecal pellets in the upper mesopelagic of the Scotia Sea, Antarctica: fecal pellet remineralization. *Limnol Oceanogr* 61:1049–1064
- Bickel SL, Tang KW (2010) Microbial decomposition of proteins and lipids in copepod versus rotifer carcasses. *Mar Biol* 157:1613–1624
- Burd AB, Hansell DA, Steinberg DK, Anderson TR and others (2010) Assessing the apparent imbalance between geochemical and biochemical indicators of meso- and bathypelagic biological activity: What the @#! is wrong with present calculations of carbon budgets? *Deep Sea Res II* 57:1557–1571
- Cervetto G, Gaudy R, Pagano M (1999) Influence of salinity on the distribution of *Acartia tonsa* (Copepoda, Calanoida). *J Exp Mar Biol Ecol* 239:33–45
- Criales-Hernández MI, Schwaborn R, Graco M, Ayón P, Hirche HJ, Wolff M (2008) Zooplankton vertical distribution and migration off Central Peru in relation to the oxygen minimum layer. *Helgol Mar Res* 62:85–100
- Daase M, Søreide JE (2021) Seasonal variability in non-consumptive mortality of Arctic zooplankton. *J Plankton Res* 43:565–585
- Daase M, Varpe Ø, Falk-Petersen S (2014) Non-consumptive mortality in copepods: occurrence of *Calanus* spp. carcasses in the Arctic Ocean during winter. *J Plankton Res* 36:129–144
- del Giorgio PA, Cole JJ (1998) Bacterial growth efficiency in natural aquatic systems. *Annu Rev Ecol Syst* 29:503–541
- del Giorgio PA, Condon R, Bouvier T, Longnecker K, Bouvier C, Sherr E, Gasol JM (2011) Coherent patterns in bacterial growth, growth efficiency, and leucine metabolism along a northeastern Pacific inshore-offshore transect. *Limnol Oceanogr* 56:1–16
- Elliott D, Harris CK, Tang KW (2010) Dead in the water: the fate of copepod carcasses in the York River estuary, Virginia. *Limnol Oceanogr* 55:1821–1834
- Escribano R, Hidalgo P (2000) Spatial distribution of copepods in the north of the Humboldt Current region off Chile during coastal upwelling. *J Mar Biol Assoc UK* 80:283–290
- Fakhraee M, Planavsky NJ, Reinhard CT (2020) The role of environmental factors in the long-term evolution of the marine biological pump. *Nat Geosci* 13:812–816
- Frangoulis C, Skliris N, Lepoint G, Elkalay K, Goffart A, Pinnegar JK, Hecq JH (2011) Importance of copepod carcasses versus faecal pellets in the upper water column of an oligotrophic area. *Estuar Coast Shelf Sci* 92:456–463
- Genin A, Gal G, Haury L (1995) Copepod carcasses in the ocean. II. Near coral reefs. *Mar Ecol Prog Ser* 123:65–71
- Glud RN, Grossart HP, Larsen M, Tang KW and others (2015) Copepod carcasses as microbial hot spots for pelagic denitrification. *Limnol Oceanogr* 60:2026–2036
- Grossart HP, Ploug H (2000) Bacterial production and growth efficiencies: direct measurements on riverine aggregates. *Limnol Oceanogr* 45:436–445
- Guidi L, Chaffron S, Bittner L, Eveillard D and others (2016) Plankton networks driving carbon export in the oligotrophic ocean. *Nature* 532:465–470
- Haines RB (1938) The effect of freezing on bacteria. *Proc R Soc B* 124:451–463
- Harding GCH (1973) Decomposition of marine copepods. *Limnol Oceanogr* 18:670–673

- Haury L, Fey C, Gal G, Hobday A, Genin A (1995) Copepod carcasses in the ocean. I. Over seamounts. *Mar Ecol Prog Ser* 123:57–63
- Hirst AG, Kiørboe T (2002) Mortality of marine planktonic copepods: global rates and patterns. *Mar Ecol Prog Ser* 230:195–209
- Iversen MH, Ploug H (2013) Temperature effects on carbon-specific respiration rate and sinking velocity of diatom aggregates—potential implications for deep ocean export processes. *Biogeosciences* 10:4073–4085
- Kiørboe T (2006) Sex, sex-ratios, and the dynamics of pelagic copepod populations. *Oecologia* 148:40–50
- Kirchman DL, Morán XAG, Ducklow H (2009) Microbial growth in the polar oceans—role of temperature and potential impact of climate change. *Nat Rev Microbiol* 7: 451–459
- Kirillin G, Grossart HP, Tang KW (2012) Modeling sinking rate of zooplankton carcasses: effects of stratification and mixing. *Limnol Oceanogr* 57:881–894
- Kok CJ, Van der Velde G (1991) The influence of selected water quality parameters on the decay rate and exoenzymatic activity of detritus of *Nymphaea alba* L. floating leaf blades in laboratory experiments. *Oecologia* 88: 311–316
- Krause KE, Dinh KV, Nielsen TG (2017) Increased tolerance to oil exposure by the cosmopolitan marine copepod *Acartia tonsa*. *Sci Total Environ* 607-608:87–94
- Lee BG, Fisher NS (1992) Decomposition and release of elements from zooplankton debris. *Mar Ecol Prog Ser* 88: 117–128
- Marsay CM, Sanders RJ, Henson SA, Pabortsava K, Achterberg EP, Lampitt RS (2015) Attenuation of sinking particulate organic carbon flux through the mesopelagic ocean. *Proc Natl Acad Sci USA* 112:1089–1094
- Mauchline J (1998) The biology of calanoid copepods. *Advances in Marine Biology*, Vol. 33. Academic Press, London
- Mazur P (1984) Freezing of living cells: mechanisms and implications. *Am J Physiol Cell Physiol* 247:C125–C142
- Middelburg JJ (2019) Marine carbon biogeochemistry: a primer for earth system scientists. Springer International Publishing, Cham
- Nedwell DB (1999) Effect of low temperature on microbial growth: lowered affinity for substrates limits growth at low temperature. *FEMS Microbiol Ecol* 30:101–111
- Pino-Pinuer P, Escribano R, Hidalgo P, Riquelme-Bugueño R, Schneider W (2014) Copepod community response to variable upwelling conditions off central-southern Chile during 2002–2004 and 2010–2012. *Mar Ecol Prog Ser* 515:83–95
- Ploug H, Kühl M, Buchholz-Cleven B, Jørgensen BB (1997) Anoxic aggregates—an ephemeral phenomenon in the pelagic environment? *Aquat Microb Ecol* 13: 285–294
- Proctor LM, Fuhrman JA (1991) Roles of viral infection in organic particle flux. *Mar Ecol Prog Ser* 69:133–142
- Rivkin RB, Legendre L (2001) Biogenic carbon cycling in the upper ocean: effects of microbial respiration. *Science* 291:2398–2400
- Robinson C (2019) Microbial respiration, the engine of ocean deoxygenation. *Front Mar Sci* 5:533
- Rysse H, Kloeters O, Germann G, Schäfer T, Wiedemann G, Oehlbauer M (2009) The antimicrobial effect of acetic acid—An alternative to common local antiseptics? *Burns* 35:695–700
- Saba GK, Steinberg DK, Bronk DA (2011) The relative importance of sloppy feeding, excretion, and fecal pellet leaching in the release of dissolved carbon and nitrogen by *Acartia tonsa* copepods. *J Exp Mar Biol Ecol* 404: 47–56
- Sampei M, Sasaki H, Hattori H, Forest A, Fortier L (2009) Significant contribution of passively sinking copepods to downward export flux in Arctic waters. *Limnol Oceanogr* 54:1894–1900
- Sampei M, Sasaki H, Forest A, Fortier L (2012) A substantial export flux of particulate organic carbon linked to sinking dead copepods during winter 2007–2008 in the Amundsen Gulf (southeastern Beaufort Sea, Arctic Ocean). *Limnol Oceanogr* 57:90–96
- Sampei M, Forest A, Fortier L, Yamamoto T, Hattori H, Sasaki H (2020) Variations in contributions of dead copepods to vertical fluxes of particulate organic carbon in the Beaufort Sea. *Mar Ecol Prog Ser* 642:67–81
- Sargent JR, Falk-Petersen S (1988) The lipid biochemistry of calanoid copepods. *Hydrobiologia* 167-168:101–114
- Sempéré R, Yoro SC, Van Wambeke F, Charrière B (2000) Microbial decomposition of large organic particles in the northwestern Mediterranean Sea: an experimental approach. *Mar Ecol Prog Ser* 198:61–72
- Steinberg DK, Landry MR (2017) Zooplankton and the ocean carbon cycle. *Annu Rev Mar Sci* 9:413–444
- Steinberg DK, Carlson CA, Bates NR, Goldthwait SA, Madin LP, Michaels AF (2000) Zooplankton vertical migration and the active transport of dissolved organic and inorganic carbon in the Sargasso Sea. *Deep Sea Res I* 47: 137–158
- Stief P, Lundgaard ASB, Morales-Ramírez Á, Thamdrup B, Glud RN (2017) Fixed-nitrogen loss associated with sinking zooplankton carcasses in a coastal oxygen minimum zone (Golfo Dulce, Costa Rica). *Front Mar Sci* 4:152
- Stief P, Lundgaard ASB, Treusch AH, Thamdrup B, Grossart HP, Glud RN (2018) Freshwater copepod carcasses as pelagic microsites of dissimilatory nitrate reduction to ammonium. *FEMS Microbiol Ecol* 94:fy144
- Stief P, Elvert M, Glud RN (2021) Respiration by ‘marine snow’ at high hydrostatic pressure: insights from continuous oxygen measurements in a rotating pressure tank. *Limnol Oceanogr* 66:2797–2809
- Tamburini C, Goutx M, Guigue C, Garel M and others (2009) Effects of hydrostatic pressure on microbial alteration of sinking fecal pellets. *Deep Sea Res II* 56: 1533–1546
- Tang KW, Elliott DT (2014) Copepod carcasses: occurrence, fate and ecological importance. In: Seuront L (ed) *Copepods: diversity, habitat and behavior*. Nova Science Publishers, Hauppauge, NY, p 255–278
- Tang KW, Hutalle KML, Grossart HP (2006a) Microbial abundance, composition and enzymatic activity during decomposition of copepod carcasses. *Aquat Microb Ecol* 45:219–227
- Tang KW, Freund CS, Schweitzer CL (2006b) Occurrence of copepod carcasses in the lower Chesapeake Bay and their decomposition by ambient microbes. *Estuar Coast Shelf Sci* 68:499–508
- Tang KW, Bickel S, Dziallas C, Grossart H (2009) Microbial activities accompanying decomposition of cladoceran and copepod carcasses under different environmental conditions. *Aquat Microb Ecol* 57:89–100
- Tang KW, Backhaus L, Riemann L, Koski M, Grossart HP, Munk P, Nielsen TG (2019a) Copepod carcasses in the

- subtropical convergence zone of the Sargasso Sea: implications for microbial community composition, system respiration and carbon flux. *J Plankton Res* 41: 549–560
- ✦ Tang KW, Ivory JA, Shimode S, Nishibe Y, Takahashi K (2019b) Dead heat: copepod carcass occurrence along the Japanese coasts and implications for a warming ocean. *ICES J Mar Sci* 76:1825–1835
- ✦ Turner JT (2015) Zooplankton fecal pellets, marine snow, phytodetritus and the ocean's biological pump. *Prog Oceanogr* 130:205–248
- ✦ Wakeham SG, Lee C, Hedges JI, Hernes PJ, Peterson MJ (1997) Molecular indicators of diagenetic status in marine organic matter. *Geochim Cosmochim Acta* 61: 5363–5369
- ✦ Wassmann P (1984) Sedimentation and benthic mineralization of organic detritus in a Norwegian fjord. *Mar Biol* 83: 83–94
- ✦ Wiedmann I, Ershova E, Bluhm BA, Nöthig EM, Gradinger RR, Kosobokova K, Boetius A (2020) What feeds the benthos in the Arctic basins? Assembling a carbon budget for the deep Arctic Ocean. *Front Mar Sci* 7:224
- ✦ Yáñez S, Hidalgo P, Tang KW (2019) Relative importance of predatory versus non-predatory mortality for dominant copepod species in the northern Chilean (23°S) Humboldt Current System. *Mar Ecol Prog Ser* 630:13–23

*Editorial responsibility: Antonio Bode,
A Coruña, Spain*

*Reviewed by: I. Fernández-Urruzola, L. Armengol
and 1 anonymous referee*

Submitted: January 21, 2021

Accepted: September 17, 2021

Proofs received from author(s): November 21, 2021